# Thermal Analysis of Power Cables Installed in Solid Bottom Trays Using an Equivalent Circuit

Shahriar Saadat, *Student Member, IEEE*, Akim Borbuev, *Student Member, IEEE*, and Francisco de León, *Fellow, IEEE*

***Abstract*—Cables in ventilated and ladder-type trays have been extensively studied and are rated according to ANSI/NEMA standards. The National Electric Code (NEC) provides guidelines on ampacity for cables installed in ventilated and ladder-type trays. However, for solid bottom trays, there is very little published material; there are neither standards nor guidelines. This paper proposes a methodological approach for the thermal rating of power cables installed in solid bottom trays with and without cover. An analog thermal–electrical circuit is derived from first thermodynamic principles. The circuit parameters are easy to compute. The method is completely general and is applicable to trays with any number of cables (not only to integer fill depths). The validity of the method is corroborated with numerous finite-element method simulations and laboratory experiments. A hand-worked example is given for illustration.**

***Index Terms*—Cable ampacity, cable thermal rating, solid bottom trays.**

## I. Introduction

CABLES are installed in solid bottom trays in schools, hospitals and retail environments [1], [2]. In some cases power generation plants and transmission and distribution substations also utilize solid bottom trays to route cables [3]. Solid bottom cable trays completely eliminate cable sagging and offer protection against dirt, dust, and rodents. Solid bottom trays (with covers) provide excellent EMI/RFI shielding protection for very sensitive circuits against external electromagnetic fields [4]. However, there are neither standards nor explicit industry guidelines on ampacity calculations for cables installed in solid bottom trays.

The pioneering work by Stolpe [5] introduced a simple method for ampacity calculations of cables installed in ventilated trays, which is the base of the current standards. Stolpe's model assumes that the cables in a tray form a composite cable mass (combination of conductive and insulating layers) of uniform depth (depth of fill) spread across the full width of the tray. The model also assumes that all cables in the tray are power cables that uniformly generate heat throughout the tray. Therefore, the cable mass consisting of various types of cables can be treated as a homogeneous rectangular mass with uniform heat generation. It is also assumed that all cables are operated at their ampacity limit (maximum load).

The study carried out in [5] used ventilated trays without cover. The effect of tray covers on cable operating temperature or ampacity was developed by Engmann [6]. It was concluded that the ampacities of cables in ventilated trays with cover are 70% to 75% of the open-top tray ampacities [6].

Uniform heat generation within cable mass was assumed in [5], [6]. Harshe and Black introduced ampacity calculation of cables in ladder type trays with and without covers with non-uniform heating within the cable pack, i.e. load diversity is taken into account [7], [8]. Harshe and Black also studied two-dimensional heat flow within the cable mass in [9].

ANSI/NEMA WC 51 ICEA P-54-440 standard [10] is based on the models established in [5], [7], [8] and provides ampacity values for cables installed in ventilated trays. A transient thermal model of cables installed in trays and ladders was developed in [11]. It was assumed that the cable bundle is located in free air. However, the calculations are limited to the cable bundle only, i.e. the heat transfer problem is solved within cable mass only. For convection and radiation calculations from the cables to ambient [11] points to [5], [6], [10].

The thermal behavior of cables installed in solid bottom trays with and without covers is reported in [3]. It follows the same procedures as [5] and [8] with a few modifications in the calculation of the effective thermal emissivity of the cable mass and tray surface to account for the solid bottom. However, the findings of [3] are not supported by experimental verification. It will be demonstrated in this paper that the method of [3] can overestimate the ampacity by up to 40%.

The National Electric Code (NEC) [12] introduces guidelines on ampacities for cables installed in ventilated trays with and without covers. In the case of solid bottom trays NEC points to Section 310.15(C). This section states that engineering supervision is necessary to compute ampacities, but no information is provided on how to evaluate the effective thermal resistance between the conductors and surroundings. Among the most popular cable ampacity programs used in the industry, including CYMCAP and USAmp+, only ETAP and AmpCalc advertise calculations for cables installed in trays. The calculations are based on [10] and therefore only applicable to ventilated trays.

To close the gap with the standards and industry guidance and practice, a methodological thermal-electrical model for ampacities of cables installed in solid bottom trays is developed in this paper. The model uses fewer assumptions than [5]–[10] and is

Manuscript received April 7, 2016; revised July 8, 2016; accepted August 17, 2016. Date of publication August 24, 2016; date of current version May 19, 2017. Paper no. TPWRD-00428-2016.

The authors are with the Department of Electrical and Computer Engineering, New York University, Brooklyn, NY 11201 USA (e-mail: ss4993@nyu.edu; ab5163@nyu.edu; fdeleon@nyu.edu).

Color versions of one or more of the figures in this paper are available online at http://ieeexplore.ieee.org.

Digital Object Identifier 10.1109/TPWRD.2016.2602184

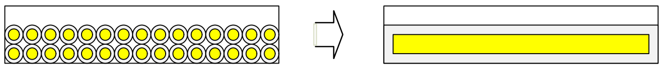

Fig. 1. Equivalent representation of cables installed in trays.

based on analytically derived heat transfer equations. Different from [3], [5]–[8] and [10], the model of this paper considers two-dimensional heat flow within the cable pack. Moreover, all previous studies combine the thermal emissivities of cable pack and tray into one effective thermal emissivity. The method proposed here treats them separately producing more accurate results. Unlike [3], [5], [7]–[10], the model proposed in this paper, accounts for the fact that the top and bottom surfaces of the cable bundle are at different temperatures. All studies based on [5] treat the cable mass as a homogeneous rectangular (infinite) slab with uniform heat generation resulting in a one-dimensional heat transfer problem whereas in the model proposed in this paper the generated heat is concentrated in an equivalent rectangular conductor (as shown in Fig. 1) yielding a more accurate two-dimensional heat transfer problem.

The proposed technique is validated with experimental measurements using a 15 kV aluminum cable and Finite Elements (FEM) simulations. The calculated ampacities show 4% to 5% differences (conservative) with respect to laboratory tests. A comparative study is made between the proposed method and [3] using the 5 kV copper cable from [10]. The validity range of the model is established with numerous FEM simulations using cables from 600 V to 35 kV. The effect of the tray surface emissivity on the cable rating is studied. A step-by-step example is presented in the Appendix to illustrate the simplicity of the method.

## II. Thermal-Electrical Circuit

Computation of the ampacity of cables installed in trays is a complex and tedious task because of the large number of cables, various loading scenarios, and cable sizes. Therefore, the following assumptions are made in the development of the circuits and models:

a) Cables are installed at a uniform depth.
b) Conductors are assumed to be at the same temperature.
c) The fill depth of the cable pack is computed as in [10]:

$$\text{Calculated Depth} = \frac{n_1 d_1^2 + n_2 d_2^2 + \cdots + n_n d_n^2}{\text{width of tray}} \quad (1)$$

where:
$d_1,\ d_2, \ldots,\ d_n$: Diameter of cables (in)
$n_1,\ n_2, \ldots,\ n_n$: Cable number with respective diameters of $d_1,\ d_2, \ldots,\ d_n$.

d) Conductors are combined to form a rectangular equivalent conductor with cross-sectional area equal to the total cross-sectional area of all conductors in the tray.
e) Temperatures of bottom and side of the tray are equal.
f) Tray has negligible thermal resistance in steady state.
g) Convection and radiation inside the tray take place between the top surface of the cable pack and the inner surface of the tray cover.

All assumptions except (d) and (e) were initially made in [5] and validated in the laboratory. Results obtained in Section VII

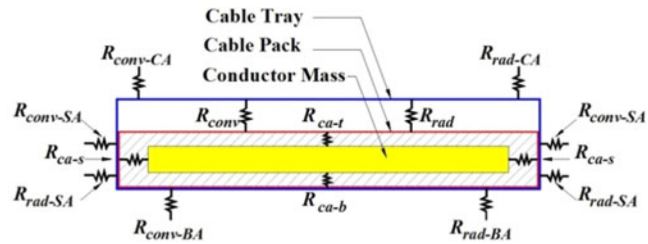


Fig. 2. Proposed model for solid bottom trays with cover.

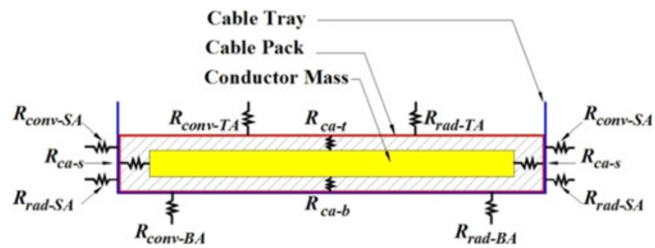


Fig. 3. Proposed model for solid bottom trays without cover.

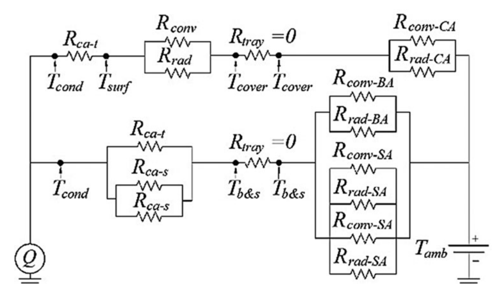


Fig. 4. Equivalent thermal-electrical circuit for cables installed in solid bottom tray with cover.

demonstrate that (d) and (e) are also reasonable and present good agreement with experiments.

With the above assumptions one can represent cables installed in trays with the equivalent model given in Fig. 1. In fact this feature of the model allows computing the ampacity of any number of cables, i.e. the model is not limited to integer fill depths. Detailed analytical models for cables installed in solid bottom trays with and without covers are presented in Figs. 2 and 3, respectively. The corresponding analog thermal-electrical circuits are given in Figs. 4 and 5. Note that in the circuit of Fig. 4 there are additional resistors in the upper branch to account for the cover and its effects on convection and radiation. The rectangular channel that represents the cable insulation and jacket has a uniform thickness. As it can be seen from Figs. 2 and 3 the presence of a tray cover results in convection and radiation inside the tray while in the case of open tray the cable pack is directly exposed to the ambient.

One can note that the circuit of Fig. 4 is more difficult to solve than the one of Fig. 5 because the cover introduces more variables. The variables used in the thermal-electrical circuits are:

$Q$: Total power losses (W/m)
$T_{cond}$: Cable conductor temperature (°K)
$T_{surf}$: Top surface temperature of cable mass (°K)

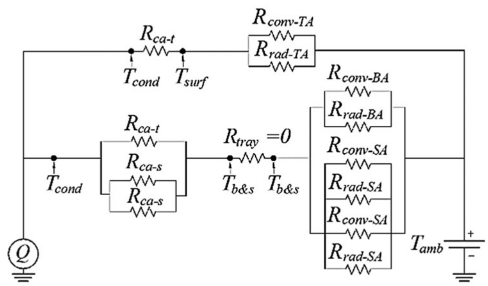


Fig. 5. Equivalent thermal-electrical circuit for cables installed in solid bottom tray without cover.

| | |
|---|---|
| $T_{cover}$: | Temperature of tray cover (°K) |
| $T_{b\&s}$: | Temperature of tray bottom and side surfaces (°K) |
| $T_{amb}$: | Ambient temperature (°K) |
| $R_{ca\,-\,t}$: | Equivalent thermal resistance between the rectangular conductor and the top or bottom surface of the cable mass (°K/W) |
| $R_{ca\,-\,s}$: | Equivalent thermal resistance between the rectangular conductor and the side surface of the cable mass (°K/W) |
| $R_{conv}$: | Equivalent thermal resistance for convection inside the covered tray (°K/W) |
| $R_{rad}$: | Equivalent thermal resistance for radiation inside the covered tray (°K/W) |
| $R_{tray}$: | Conductive thermal resistance of tray (°K/W) |
| $R_{conv\,-\,BA}$: | Equivalent thermal resistance for convection over the bottom of tray (°K/W) |
| $R_{rad\,-\,BA}$: | Equivalent thermal resistance for radiation over the bottom of tray (°K/W) |
| $R_{conv\,-\,CA}$: | Equivalent thermal resistance for convection over the tray cover (°K/W) |
| $R_{rad\,-\,CA}$: | Equivalent thermal resistance for radiation over the tray cover (°K/W) |
| $R_{conv\,-\,SA}$: | Equivalent thermal resistance for convection over the tray side (°K/W) |
| $R_{rad\,-\,SA}$: | Equivalent thermal resistance for radiation over the tray side (°K/W) |
| $R_{conv\,-\,TA}$: | Equivalent thermal resistance for convection over the top of cable pack when there is no cover (°K/W) |
| $R_{rad\,-\,TA}$: | Equivalent thermal resistance for radiation over the top of the cable pack when there is no cover (°K/W) |

## III. Thermodynamics (Heat Transfer)

The heat transfer from the conductors to the surroundings takes place through conduction, convection, and radiation.

### A. Conduction

Heat transfer by conduction takes place within the cable mass. The two-dimensional thermal resistance for conduction is computed using [13]:

$$R_{cond} = \frac{1}{Sk} \tag{2}$$

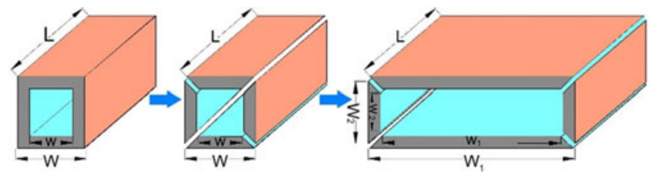


Fig. 6. Two-dimensional heat flow in a square channel [13] and partitioned cable mass for conduction shape factor calculation.

where:

| | |
|---|---|
| $R_{cond}$ | Thermal resistance for conductive heat transfer (°K/W) |
| $S$ | Conduction shape factor (m) |
| $k$ | Thermal conductivity (W/m·°K) |

The conduction shape factor depends on the geometry of the solid body. Yovanovich [14] presents a general expression for computing the conduction shape factor. Conduction shape factors for various geometries can be found in [13]–[17].

Analytical formulae for the calculation of the conduction shape factors for a square channel (the channel can be a solid body) shown in Fig. 6 are [13]:

$$\frac{W}{w} < 1.4 \quad \rightarrow \quad S = \frac{2\pi L}{0.785 \ln\left(\frac{W}{w}\right)} \tag{3}$$

$$\frac{W}{w} > 1.4 \quad \rightarrow \quad S = \frac{2\pi L}{0.930 \ln\left(\frac{W}{w}\right) - 0.050} \tag{4}$$

For $W/w = 1.4$, (3) and (4) give almost the same values. As it can be seen from Figs. 2 and 3, the cable pack composed of insulation and jacket forms a rectangular shell. This shell is partitioned into four sections as illustrated in Fig. 6. Conduction shape factors in (3) and (4) are for a complete shape, therefore, as it is shown in [14]–[17] for a quarter of the rectangular shell, the conduction shape factors (3) and (4) should be modified as follows:

$$\frac{W}{w} < 1.4 \quad \rightarrow \quad S = \frac{\left(\frac{\pi}{2}\right) L}{0.785 \ln\left(\frac{W}{w}\right)} \tag{5}$$

$$\frac{W}{w} > 1.4 \quad \rightarrow \quad S = \frac{\left(\frac{\pi}{2}\right) L}{0.930 \ln\left(\frac{W}{w}\right) - 0.050} \tag{6}$$

The conduction shape factor is calculated for each section separately using (5) and (6). Finally conductive thermal resistances between the conductor mass and top, bottom and sides of the cable pack utilizing (2) are computed.

### B. Convection

Heat transfer by convection is characterized by a convective heat coefficient as follows [13]:

$$h_{conv} = \frac{k_{air} \cdot Nu}{L} \tag{7}$$

where:

| | |
|---|---|
| $h_{conv}$ | Convective heat transfer coefficient (W/m$^2$·°K) |
| $k_{air}$ | Thermal conductivity of air (W/m·°K) |
| $Nu$ | Nusselt number |
| $L$: | Characteristic length (m) |

The equivalent thermal resistance for convection is computed using the following expression [13]:

$$R_{conv} = \frac{1}{h_{conv} \cdot A} \tag{8}$$

where:

$R_{conv}$: Thermal resistance for convective heat transfer (°K/W)

$A$: Area of convecting surface (m$^2$)

*1) Convection Inside the Tray:* The Nusselt number depends on the geometry of the convective system. Convection inside the tray is determined by the following equation [13]:

$$Nu = 0.069 Ra^{1/3}\, Pr^{0.074} \tag{9}$$

$Ra$ is Rayleigh number and $Pr$ is Prandtl number which have the following expressions [13]:

$$Ra = \frac{g\beta(T_1 - T_2)L^3}{\alpha\nu} \tag{10}$$

$$\beta = \frac{1}{T_f} \tag{11}$$

$$T_f = \frac{T_1 + T_2}{2} \tag{12}$$

$$\alpha = \frac{k}{\rho \cdot C_p} \tag{13}$$

$$k = 1.5207 \cdot 10^{-11} \cdot T_f^3 - 4.8574 \cdot 10^{-8} \cdot T_f^2 + 1.018 \cdot 10^{-4} \cdot T_F - 3.9333 \cdot 10^{-4} \tag{14}$$

$$\rho = \frac{p}{R \cdot T_f} \tag{15}$$

$$\nu = \mu/\rho \tag{16}$$

$$\mu = \frac{C_1 \cdot {T_f}^{3/2}}{T_f + C_2} \tag{17}$$

$$Pr = \frac{\mu C_p}{k} \tag{18}$$

where:

$g$ Acceleration of gravity ($g = 9.81\,\mathrm{m/s^2}$)
$\beta$ Volumetric thermal expansion coefficient (1/°K)
$T_f$ Film temperature (°K)
$T_1$ Temperature of hot surface (°K)
$T_2$ Temperature of cool surface (°K)
$\alpha$ Thermal diffusivity at $T_f$ (m$^2$/s)
$\nu$ Kinematic viscosity at $T_f$ (m$^2$/s)
$\mu$ Dynamic viscosity at $T_f$ (kg/m·s)
$\rho$ Density of air at $T_f$ (kg/m$^3$)
$p$ Atmospheric pressure ($p = 101\ \ 325\,\mathrm{Pa}$)
$R$ Gas constant for dry air ($R = 287.058\,\mathrm{J/\,kg \cdot {}^\circ K}$)
$C_p$ Specific heat capacity at constant pressure ($C_p = 1006\,\mathrm{J/\,kg \cdot {}^\circ K}$)
$C_1$ Sutherland viscosity law coefficient ($C_1 = 1.458 \cdot 10^{-6}\ \mathrm{kg/m \cdot s \cdot {}^\circ K^{1/2}}$)
$C_2$ Sutherland viscosity law coefficient ($C_2 = 110.4\ {}^\circ\mathrm{K}$)

*2) Convection at the Bottom and Cover of Tray:* For horizontal surfaces the Nusselt number is defined as follows [13]:

$$Nu = C \cdot Ra^m \tag{19}$$

For the upper surface: $C = 0.54$ and $m = 0.25$; for the lower surface: $C = 0.27$ and $m = 0.25$.

*3) Convection on the Sides of Tray:* In case of vertical surfaces the Nusselt number is given by [13]:

$$Nu = 0.68 + \frac{0.670 Ra^{1/4}}{\left[1 + (0.492/Pr)^{9/16}\right]^{4/9}} \tag{20}$$

### C. Radiation

Radiation takes place in the tray between the top surface of the cable pack and the tray cover and then from the tray outer surfaces to ambient.

*1) Radiation Within the Tray:* Since the tray is covered, radiation inside the tray happens between the top surface of cable mass and the inner surface of the cover. This exchange depends strongly on the surface geometry and orientation, as well as on the surface emissivity and temperature. The concept of view factor is used to compute radiation exchange between any two surfaces [13].

The following view factor is used for a covered cable tray which yields a system of two rectangular surfaces of equal size in opposite location [6]:

$$F = \frac{\varepsilon_{cable}\varepsilon_{tray}}{3.2 - \varepsilon_{cable} - \varepsilon_{tray}} \tag{21}$$

Radiative heat transfer coefficient and thermal resistance are given by [6]:

$$h_{rad} = F\sigma\left(T_1^2 + T_2^2\right)(T_1 + T_2) \tag{22}$$

$$R_{rad} = \frac{1}{h_{rad} \cdot A} \tag{23}$$

where:

$F$ Radiation view factor
$\varepsilon_{cable}$ Surface emissivity of cable pack
$\varepsilon_{tray}$ Surface emissivity of tray
$h_{rad}$ Radiative heat transfer coefficient (W·m$^{-2}$·°K$^{-1}$)
$\sigma$ Stephen-Boltzmann constant ($\sigma = 5.67 \times 10^{-8}$W/m$^2$ · °K)
$T_1$ Temperature of emitting surface (°K)
$T_2$ Temperature of absorbing surface (°K)
$R_{rad}$ Thermal resistance for radiative heat transfer (°K/W)
$A$ Surface area (m$^2$)

*2) Radiation on Outer Surfaces of Tray:* Radiative processes that occur at the surface are described by [13]:

$$h_{rad} = \varepsilon_{tray}\sigma\left(T_1^2 + T_2^2\right)(T_1 + T_2) \tag{24}$$

$$R_{rad} = \frac{1}{h_{rad} \cdot A} \tag{25}$$

## IV. Solving the Thermal–Electrical Circuit

The proposed model is based on the equivalent thermal-electrical circuits of Figs. 4 and 5.

### A. Cables Installed in Solid Bottom Trays With Covers

The following system of equations can be derived from the circuit for solid bottom trays with covers applying KVL:

$$T_{cond} = T_{surf} + Q_t \cdot R_1 \tag{26}$$

$$T_{surf} = T_{cover} + Q_t \cdot R_2 \tag{27}$$

$$T_{cover} = T_{amb} + Q_t \cdot R_3 \tag{28}$$

$$T_{cond} = T_{b\&s} + \frac{Q_b \cdot R_1}{2} + \frac{Q_s \cdot R_5}{2} \tag{29}$$

$$T_{b\&s} = T_{amb} + Q_b \cdot R_4 \tag{30}$$

$$T_{b\&s} = T_{amb} + Q_s \cdot R_6 \tag{31}$$

where:

$Q_t$ Heat flow in upper direction (W)
$Q_b$ Heat flow in lower direction (W)
$Q_s$ Heat flow to the sides (W)
$R_1$ $R_{ca-t}$
$R_2$ $R_{conv}||R_{rad}$
$R_3$ $R_{conv-CA}||R_{rad-CA}$
$R_4$ $R_{conv-BA}||R_{rad-BA}$
$R_5$ $R_{ca-s}/2$
$R_6$ $(R_{conv-SA}||R_{rad-SA})/2$

The given system of equations is non-linear due to the nature of the convection and radiation that depend on temperature. The only known parameters of the system of equations are the conductor and ambient temperatures. Note that thermal resistances for conduction are constant while thermal resistances for convection and radiation are temperature-dependent and computed accordingly. To solve such system of equations iterative methods are required. The successive relaxation method is utilized as in [18]. The relaxation parameter $\lambda = 0.5$ is used to obtain the best results. The iterative method is described in the following steps:

1) Start with reasonable initial guesses for $T_{cover}(0)$ and $T_{b\&s}(0)$, which are used to evaluate $Q_t(0)$, $Q_b(0)$ and $Q_s(0)$ from (28), (30) and (31), respectively
2) Compute $T_{surf}(0)$ using (26)
3) Determine $Q_t(1)$ solving (27)
4) Use $Q_t(1)$ to calculate new values for $T_{cover}(1)$ and $T_{b\&s}(1)$ from linear combinations of the previous value and the one computed with (28) and (29) as follows:

$$T_{cover}(1) = (1-\lambda)\, T_{cover}(0) + \lambda\,(T_{amb} + Q_t(1) \cdot R_3) \tag{32}$$

$$T_{b\&s}(1) = (1-\lambda)\, T_{b\&s}(0) + \lambda\left(T_{cond} - \frac{Q_b(0) \cdot R_1}{2} - \frac{Q_s(0) \cdot R_5}{2}\right) \tag{33}$$

5. Find the errors:

$$E_{cover}(1) = T_{cover}(1) - T_{cover}(0) \tag{34}$$

$$E_{b\&s}(1) = T_{b\&s}(1) - T_{b\&s}(0) \tag{35}$$

6. If the errors are greater than 0.5 °C repeat the steps.

The objective of these iterations is to determine the total heat generated $Q$ in Watts per unit of length.

$$Q = Q_t + Q_b + Q_s \tag{36}$$

Applying Joule's law, the ampacity of the cable can be computed from:

$$I = \sqrt{\frac{Q}{nR_{ac}}} \tag{37}$$

where:

$I$ Ampacity of cables (A)
$Q$ Heat generated in the cables (W/m)
$n$ Number of cables
$R_{ac}$ ac resistance of the conductor at the operating temperature (Ω/m)

### B. Cables Installed in Solid Bottom Trays Without Covers

The system of equations in the case of solid bottom trays without covers is:

$$T_{cond} = T_{surf} + Q_t \cdot R_1 \tag{38}$$

$$T_{surf} = T_{amb} + Q_t \cdot R_7 \tag{39}$$

$$T_{cond} = T_{b\&s} + \frac{Q_b \cdot R_1}{2} + \frac{Q_s \cdot R_5}{2} \tag{40}$$

$$T_{b\&s} = T_{amb} + Q_b \cdot R_4 \tag{41}$$

$$T_{b\&s} = T_{amb} + Q_s \cdot R_6 \tag{42}$$

where:

$R_7$ $R_{conv-TA}||R_{rad-TA}$

The solution of the system of equations (38)–(42) follows the same procedure described in the previous section except that there are fewer unknowns and equations.

## V. Laboratory Tests

A single core 350 kcmil, aluminum conductor, 15 kV EPR insulated, PVC jacket, copper tape shield cable was used in the laboratory experiments. The cable has a measured outside diameter of 36.2 mm (1.425 in). The cable tray used in the experiments is made of galvanized steel, 3.048 m (10 ft) long, 0.6096 m (24 in) wide, 0.1016 m (4 in) height and thickness of 1.5 mm.

### A. One Inch Fill Depth

The first experiment was conducted using twelve cables corresponding to a fill depth of slightly larger than one inch as per ICEA/NEMA; see (1). The cables were connected in series and looped back and forth so that they can be fed from one source. The total length of the cables is 120 ft.

The thermal behavior of the conductors and jackets were measured with thermocouples and monitored from a computer. The locations of the thermocouples ($T_N$) are the same for both open and covered tray tests (see Fig. 7). The experimental setup is shown in Fig. 8(a). For illustration purposes the cover is removed. The ambient air temperature was measured as 23 °C and 24 °C for open and covered trays, respectively. The experiments

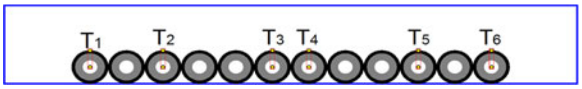


Fig. 7. Locations of thermocouples for the one-inch depth experiment. Note that there are two thermocouples per location, one touching the jacket and one touching the conductor.

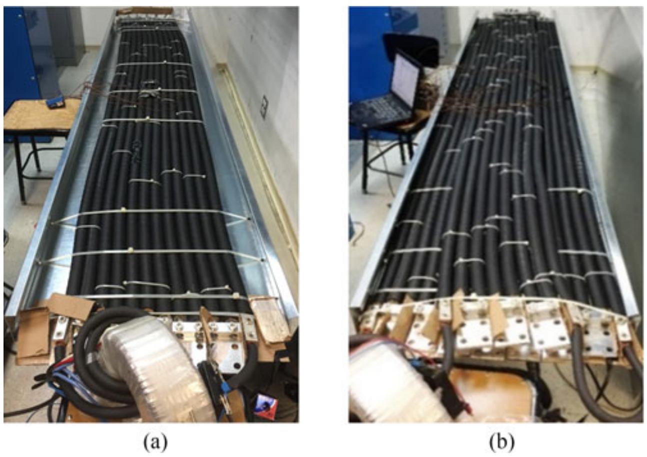


Fig. 8. Experimental setup for one inch (a) and two inch (b) tests.

TABLE I
CURRENT & HST COMPARISON FOR ONE INCH FILL DEPTH

| Tray Installation | Current (A) | | | HST Rise (°C) | | |
|---|---|---|---|---|---|---|
| | Experiment & FEM | Proposed Model | Difference (%) | Experiment & Proposed Model | FEM | Difference (%) |
| Open | 371 | 390 | 5.1 | 72 | 76 | 5.6 |
| Covered | 296 | 292 | 1.4 | 99 | 97 | 2.0 |

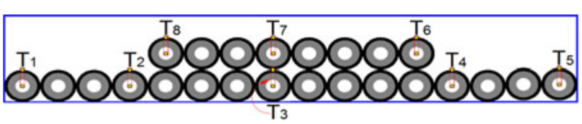


Fig. 9. Locations of thermocouples for the two-inch experiment. Note that there are two thermocouples per location, one touching the jacket and one touching the conductor.

ran for 15.5 (open tray) and 17.5 hours (covered tray) until the temperature reached steady-state. The results are presented in Table I.

### B. Two Inch Fill Depth

Twenty four cables were tightly packed with a fill depth of 2.03 inches as depicted in Fig. 8(b). Again for illustration purposes the cover is removed. Thermocouple locations are shown in Fig. 9. The ambient air temperature was recorded as 23 °C for both open and covered trays. Eleven hours (open tray) and 25 hours (covered tray) were required to make sure that the temperatures reached steady-state; see Table II.

TABLE II
CURRENT & TEMPERATURE COMPARISON FOR TWO INCH FILL DEPTH

| Tray Installation | Current (A) | | | HST Rise (°C) | | |
|---|---|---|---|---|---|---|
| | Experiment & FEM | Proposed Model | Difference (%) | Experiment & Proposed Model | FEM | Difference (%) |
| Open | 230 | 220 | 4.3 | 60 | 63 | 5.0 |
| Covered | 171 | 155 | 9.0 | 56 | 59 | 5.4 |

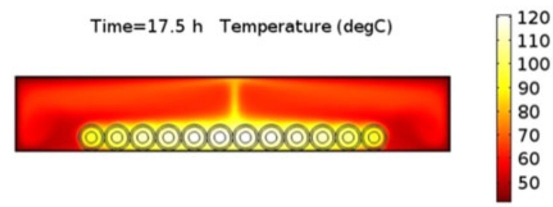


Fig. 10. Steady state temperature distribution for one inch fill depth with cover.

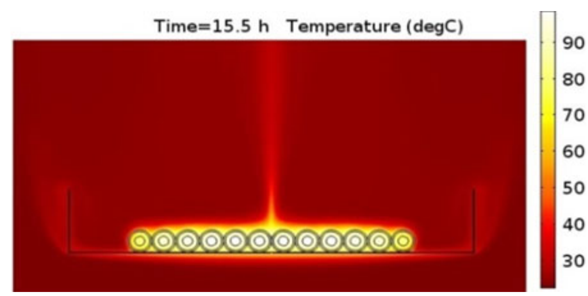


Fig. 11. Steady state temperature distribution for one inch fill depth without cover.

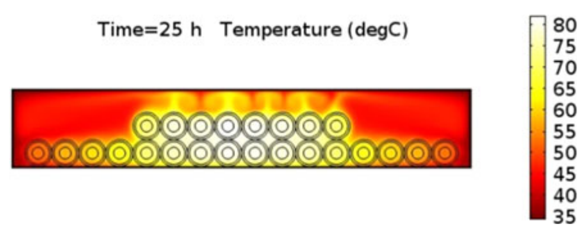


Fig. 12. Steady state temperature distribution for two inch fill depth with cover.

## VI. FEM MODEL

COMSOL Multiphysics, Finite Elements Method (FEM) software is used to evaluate the experimental results in terms of final temperatures. The software solves the complete computational fluid dynamics, nonlinear electromagnetic, and heat transfer equations simultaneously by coupling Heat Transfer, Fluid Flow, and Electromagnetic multi-physics packages.

Figs. 10–13 provide the steady-state temperature distribution obtained from FEM simulations with and without covers for one and two inch-fill depths, respectively. The purpose of the simulations is to reproduce laboratory tests for one and two inch-fill

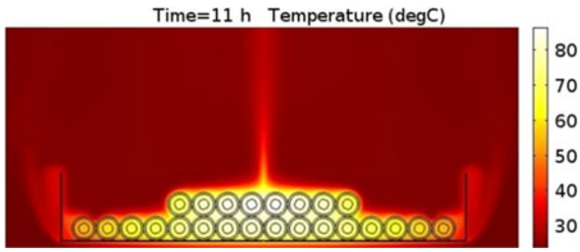


Fig. 13. Steady state temperature distribution for two inch fill depth without cover.

TABLE III
ALLOWABLE HEAT INTENSITIES OF VENTILATED VS. SOLID BOTTOM TRAYS WITHOUT COVERS; REPRODUCED FROM [3]

| Fill Depth of Cables (in) | Allowable Heat Intensity (W/ft·in$^2$) | | Derating Factor |
|---|---|---|---|
| | Ventilated [3] | Solid Bottom | |
| 1 | 5.925 | 5.257 | 0.942 |
| 1.5 | 3.557 | 3.186 | 0.946 |
| 2 | 2.427 | 2.194 | 0.951 |
| 2.5 | 1.784 | 1.624 | 0.954 |
| 3 | 1.377 | 1.26 | 0.957 |

TABLE IV
ALLOWABLE HEAT INTENSITIES OF VENTILATED VS. SOLID BOTTOM TRAYS WITH COVERS; REPRODUCED FROM [3]

| Fill Depth of Cables (in) | Derating for Solid Bottom Tray without Covers | Additional Derating to account for Cover | Total Derating for Solid Bottom Trays with Covers |
|---|---|---|---|
| 1 | 0.942 | 0.72 | 0.68 |
| 2 | 0.951 | 0.74 | 0.70 |
| 3 | 0.957 | 0.77 | 0.74 |

TABLE V
CALCULATED AMPACITIES FOR A SINGLE CORE 250 KCMIL, COPPER CONDUCTOR, 5 KV SHIELDED CABLE

| Fill Depth of Cables (in) | Calculated Cables (in) Ampacity (A) | | | | | |
|---|---|---|---|---|---|---|
| | Open | | | Covered | | |
| | Using [3] | Proposed Model | Difference (%) | Using [3] | Proposed Model | Difference (%) |
| 1 | 314 | 280 | 12.3 | 267 | 191 | 39.7 |
| 1.5 | 244 | 215 | 13.5 | N/A | 154 | N/A |
| 2 | 202 | 177 | 14.0 | 174 | 131 | 32.6 |
| 2.5 | 173 | 152 | 13.7 | N/A | 116 | N/A |
| 3 | 153 | 133 | 14.7 | 134 | 104 | 28.8 |

depths and validate the FEM model. The experiments have run until the temperature in the system reaches the steady-state. It has been observed that due to the large number of highly non-linear equations solved by the software, simulation of 11 to 25 hours of actual cable transient response, could take from several hours up to weeks using a server that has 24 cores in its central processing unit (CPU) running at 3.33 GHz each as well as 96 GB of DDR3 random-access memory (RAM). For this reason the advantage of the closed system in covered tray simulations was utilized. COMSOL Multiphysics has a feature that allows defining external natural convection and radiation on the outer surfaces of the covered tray, thus dramatically decreasing the simulation time. This feature uses much simpler algebraic equations rather than partial differential equations. Therefore, although the region outside the tray with cover is not illustrated (see Figs. 10 and 12), it is physically present and represented by natural convection and radiation on the boundaries of the system. The Tables I to II show a good match of the hot spot temperatures (HST's) between laboratory experiments and FEM simulations. FEM simulations yield a maximum difference of 5.6% when compared to experiments.

## VII. EVALUATION OF THE PROPOSED MODEL

In this section the evaluation of the proposed model and validation of the thermal-electrical circuit are carried out. The results given in Tables I and II are obtained in the following way:

1) The HST measured in the experiment is entered as data in the model and the current is computed. Therefore, the HSTs of experiments and model are the same and the currents are slightly different (by a few percent).
2) For FEM simulations the current applied in the experiment is used as the input data and the temperature is computed. Therefore, currents of the laboratory tests and FEM simulations are the same and the temperatures show a small difference.

All differences between calculated and measured parameters are within engineering accuracy (2% to 9%). Note that the percent difference in the temperatures are calculated based on the temperature rise above the ambient temperature (24 °C for one inch fill depth with cover, 23 °C for one inch fill depth with no cover and two inch fill depth with both cover and no cover). For instance, from Table I for one inch fill depth with no cover, the difference is computed between 72 °C (Experiment & Model) and 76 °C (FEM). A detailed example for two inch fill depth with cover is provided in the Appendix.

## VIII. CALCULATED AMPACITIES AND EVALUATION OF [3]

As it was mentioned in the Introduction, the study of [3] suggests that the ampacities provided in [10] need to be reduced when solid bottom trays are utilized. The derating factors are given in terms of allowable heat generation $q$ (see Tables III and IV). The ampacity is calculated using the following expression [10]:

$$I = d \times \sqrt{q/(nR_{ac})} \tag{43}$$

where:

$I$: Ampacity of a cable (A)
$d$: Cable diameter (in)
$q$: Allowable heat generation (W/ft·in$^2$)
$n$: Number of cables

TABLE VI
VALIDITY RANGE OF THE MODEL FOR 600 V CABLES

| Fill Depth of Cables (in) | 1/0 AWG HST (°C) | 1/0 AWG Current (A) FEM | Model | Diff. (%) | 500 kcmil HST (°C) | 500 kcmil Current (A) FEM | Model | Diff. (%) |
|---|---|---|---|---|---|---|---|---|
| 1 | 83 | 65 | 60 | 7.7 | 103 | 308 | 303 | 1.6 |
| 2 | – | – | – | – | 102 | 209 | 208 | 0.5 |
| 3 | – | – | – | – | 96 | 150 | 158 | 5.3 |

TABLE VII
VALIDITY RANGE OF THE MODEL FOR 2 kV CABLES

| Fill Depth of Cables (in) | 1/0 AWG HST (°C) | 1/0 AWG Current (A) FEM | Model | Diff. (%) | 500 kcmil HST (°C) | 500 kcmil Current (A) FEM | Model | Diff. (%) |
|---|---|---|---|---|---|---|---|---|
| 1 | 82 | 66 | 61 | 7.6 | 90 | 277 | 277 | 0.0 |
| 2 | – | – | – | – | 88 | 192 | 187 | 2.6 |
| 3 | – | – | – | – | 90 | 153 | 153 | 0.0 |

TABLE VIII
VALIDITY RANGE OF THE MODEL FOR 5 kV CABLES

| Fill Depth of Cables (in) | 2 AWG HST (°C) | 2 AWG Current (A) FEM | Model | Diff. (%) | 500 kcmil HST (°C) | 500 kcmil Current (A) FEM | Model | Diff. (%) |
|---|---|---|---|---|---|---|---|---|
| 1 | 81 | 55 | 51 | 7.3 | 92 | 308 | 314 | 1.9 |
| 2 | – | – | – | – | 91 | 212 | 214 | 0.9 |
| 3 | – | – | – | – | 90 | 169 | 169 | 0.0 |

$R_{ac}$: ac resistance of the conductor at the operating temperature ($\mu\Omega$/ft)

Note that the allowable heat generation $q$ is given in Watts per unit volume while the heat generated by the cables $Q$ in (30) is given in Watts per unit length. This difference is reflected in the ampacity formulae (30) and (36); the ampacity in (36) is directly proportional to the cable diameter while the ampacity in (30) is related to the cable diameter through the heat generated $Q$ in the system.

To obtain ampacity tables for cables installed in solid bottom trays based on the proposed model and assess the results given in [3] a comparison between the two methods is presented in Table V. Due to space limitations, Table V is based on only one cable type. The single core 250 kcmil, copper conductor, 5 kV, shielded power cable from [10], Tables 5–18 is used. The cable has an outside diameter of 25.4 mm (1.0 in), as an example twenty four of these cables are used to fill one inch fill depth.

The derating factors in Tables III and IV apply to the allowable heat intensity. Therefore, the ampacity values in [10] need to

TABLE IX
VALIDITY RANGE OF THE MODEL FOR 15 kV CABLES

| Fill Depth of Cables (in) | 2 AWG HST (°C) | 2 AWG Current (A) FEM | Model | Diff. (%) | 500 kcmil HST (°C) | 500 kcmil Current (A) FEM | Model | Diff. (%) |
|---|---|---|---|---|---|---|---|---|
| 1 | 82 | 69 | 64 | 7.2 | 94 | 332 | 344 | 3.6 |
| 2 | – | – | – | – | 90 | 228 | 228 | 0.0 |
| 3 | – | – | – | – | 90 | 181 | 181 | 0.0 |

TABLE X
VALIDITY RANGE OF THE MODEL FOR 25 kV AND 35 kV CABLES

| Fill Depth of Cables (in) | 1/0 AWG HST (°C) | 1/0 AWG Current (A) FEM | Model | Diff. (%) | 350 kcmil HST (°C) | 350 kcmil Current (A) FEM | Model | Diff. (%) |
|---|---|---|---|---|---|---|---|---|
| 1 | 84 | 128 | 119 | 7.0 | 98 | 302 | 322 | 6.6 |
| 2 | – | – | – | – | 82 | 206 | 191 | 7.3 |
| 3 | – | – | – | – | 84 | 162 | 155 | 4.3 |

be multiplied by the square root of the corresponding derating factor from Tables III and IV to account for the solid bottom of the tray. Conductor operating and ambient temperatures are 90 °C and 40 °C, respectively.

The differences between the two methods in Table V were computed with respect to the ampacity determined using the proposed model. One can note that in the open tray installations the differences are from 12% to 15% for this particular cable. For covered tray installations the differences grows larger from 28% to 40%. One must conclude that the method of reference [3] overestimates the ampacity excessively.

## IX. VALIDITY RANGE OF THE PROPOSED MODEL

This section obtains the validity range of the model. Since solid bottom trays are utilized in low and medium voltage applications, cables from 600 V to 35 kV are evaluated. The study is carried out on the cables given in [10] by comparing FEM simulations and the model in terms of the calculated current, i.e. the final temperatures of the two methods are the same. Because [10] provides the ampacity of cables up to 15 kV only, cables from the General Cable catalogue rated 25 kV and 35 kV are also selected [19].

It is worth mentioning that FEM simulations take a long time to reach the steady state due to the complexity of natural convection of free air. For this reason, for small size cables (lower limits) FEM simulations are performed for one inch of cables while for large size cables (upper limits) the model and FEM simulations are compared for one, two and three inch fill depths. Additionally, the evaluation is done on covered tray installations only. The ambient temperature is 40 °C as in [10].

TABLE XI
EFFECT OF TRAY SURFACE EMISSIVITY ON RATING OF CABLES IN SOLID BOTTOM TRAYS WITH COVERS

| Fill Depth of Cables (in) | Calculated Ampacity (A) | | |
|---|---|---|---|
| | Surface Emissivity of Tray | | |
| | $\epsilon = 0.23$ | $\epsilon = 0.88$ | Ampacity Increase (%) |
| 1 | 166 | 217 | 30.7 |
| 2 | 115 | 145 | 26.1 |
| 3 | 91 | 113 | 24.2 |
| 4 | 78 | 93 | 19.2 |

TABLE XII
EFFECT OF TRAY SURFACE EMISSIVITY ON RATING OF CABLES IN SOLID BOTTOM TRAYS WITHOUT COVERS

| Fill Depth of Cables (in) | Calculated Ampacity (A) | | |
|---|---|---|---|
| | Surface Emissivity of Tray | | |
| | $\varepsilon = 0.23$ | $\varepsilon = 0.88$ | Ampacity Increase (%) |
| 1 | 256 | 271 | 5.9 |
| 2 | 159 | 169 | 6.3 |
| 3 | 119 | 128 | 7.6 |
| 4 | 96 | 103 | 7.3 |

Tables VI–X present the results for the lower and upper limits of the validity range of the model.

The conclusions of this study are: (1) for 600 V and 2 kV cables the method is valid from 1/0 AWG to 500 kcmil; (2) for 5 kV and 15 kV cables the method works well from 2 AWG to 500 kcmil; (2) for 25 kV and 35 kV cables the model is valid from 1/0 AWG to 350 kcmil.

## X. EFFECT OF TRAY SURFACE EMISSIVITY ON RATING OF CABLES IN SOLID BOTTOM TRAYS

New galvanized steel trays tend to be shiny and have low surface emissivity ($\epsilon_{\text{new}} = 0.23$). On the other hand, old galvanized steel trays are matte and have high surface emissivity ($\epsilon_{\text{old}} = 0.88$) [20]. To analyze the effects of the tray surface emissivity on the cable ratings, the cable studied in Section VIII is used to obtain the values given in Tables XI and XII for trays with and without covers. The ampacity percent increase is computed between the two cases, i.e. $\epsilon_{\text{new}} = 0.23$ and $\epsilon_{\text{old}} = 0.88$ for a given fill depth of the cables.

The results clearly show that there are important advantages of using trays with high surface emissivity. One can see that for covered installations having the tray painted in a matte color can increase the ampacity from 6% for trays with no cover and as much as 30% for trays with cover.

## XI. CONCLUSION

A methodological model has been proposed for the calculation of ampacity of cables installed in solid bottom trays with and without covers. The technique is completely general and allows for the calculation of ampacities of any number of cables, i.e. the model is not limited to integer fill depths. The accuracy of the model has been verified with experimental results and FEM simulations. The validity range of the model has been established and the effect of tray surface emissivity on the cable ampacity has been analyzed.

Since there is little published data on the subject the results of this research can be used as a basis for establishing standard or guidelines for the calculation of ampacities of cables installed in solid bottom trays with and without covers.

TABLE XIII
INPUT & CALCULATED DATA

| Parameter | Description | Value |
|---|---|---|
| $\lambda$ | Relaxation parameter | 0.5 |
| $w$ | Width of tray | 0.6096 |
| $ht$ | Depth of tray | 0.1016 |
| $d_{cond}$ | Conductor diameter | 0.0156 |
| $d_{ins}$ | Insulation diameter | 0.0304 |
| $d_{cable}$ | Overall cable diameter | 0.0362 |
| $L$ | Length of cable/tray | 3.048 |
| $A_h$ | Surface area of the tray cover and bottom | 1.8581 |
| $A_v$ | Surface are of the tray sides | 0.3097 |
| $pd$ | Characteristic length for convection over tray cover and bottom (area/perimeter) | 0.2540 |
| $th$ | Thickness of rectangular shell that represents insulation and jacket | 0.0217 |
| $w_1$ | Width of equivalent rectangular conductor | 0.5662 |
| $w_2$ | Height of equivalent rectangular conductor | 0.0082 |
| $R_{ndc}$ ($\Omega$/m) | Nominal dc resistance of the conductor at 20 °C | $1.624 \cdot 10^{-4}$ |
| $R_{dc}$ ($\Omega$/m) | dc resistance of the conductor with 2% of stranding factor at 20 °C | $1.65648 \cdot 10^{-4}$ |
| $R_{ac}$($\Omega$) | ac resistance of the conductor 3.048 meter long at the operating temperature | $6.2814 \cdot 10^{-4}$ |
| $k_{ins}$ | Thermal conductivity of EPR insulation | 0.2 |
| $k_{jack}$ | Thermal conductivity of PVC jacket | 0.2 |
| $\varepsilon_{pvc}$ | Thermal emissivity of PVC jacket | 0.9 |
| $\varepsilon_{tray}$ | Thermal emissivity of galvanized steel tray (new) | 0.2 |
| $F$ | View factor for radiation inside tray; see (21) | 0.0857 |
| $T_{core}$ | Conductor temperature | 79.0 |
| $T_{amb}$ | Ambient temperature | 23.0 |
| $T_{cover}$ | Initial value for temperature of tray cover | 28.0 |
| $T_{b\&s}$ | Initial temperature of tray sides and bottom | 28.0 |

## APPENDIX

Illustration of the proposed model is provided through a numerical example based on two inch fill depth with cover. Table XIII provides input and calculated data. Table XIV presents the solution of the system of equations (26)–(31) with parameters calculated at each iteration. The initial values are ambient temperature plus 5 °C. All parameters are given in SI units except the temperature which is presented in °C for convenience. Nominal dc resistance and stranding factor of 8000 series aluminum compact conductor are in accordance with ASTM Specs B800 and B801 and ICEA Part 2, Sections 2.1 and 2.5 as indicated in the cable specs sheet. The ac resistance of the conductor is computed as per IEC 60287-1-1 Sections 2.1.2 and 2.1.4.1 and adjusted to the operating temperature.

TABLE XIV
SOLUTION OF TWO INCH FILL DEPTH WITH COVER

| Parameter | Equation | Iteration Number | | | | |
|---|---|---|---|---|---|---|
| | | 0 | 1 | ... | 9 | 10 |
| | | Step 1 | | | | |
| $T_{cover}$ | (25) | 28.0 | 46.0 | ... | 39.9 | 39.9 |
| $T_{b\&s}$ | (26) | 28.0 | 49.8 | ... | 41.9 | 42.5 |
| $T_{f-CA}$ | (12) | 25.5 | 34.5 | ... | 31.5 | 31.5 |
| $\beta_{CA}$ | (11) | 0.0033 | 0.0033 | ... | 0.0033 | 0.0033 |
| $\rho_{CA}$ | (15) | 1.1819 | 1.1473 | ... | 1.1587 | 1.1587 |
| $k_{CA}$ | (14) | 0.0261 | 0.0268 | ... | 0.0266 | 0.0266 |
| $\mu_{CA}$ | (17) | $18.4{\cdot}10^{-6}$ | $18.8{\cdot}10^{-6}$ | ... | $18.7{\cdot}10^{-6}$ | $18.7{\cdot}10^{-6}$ |
| $\nu_{CA}$ | (16) | $15.6{\cdot}10^{-6}$ | $16.4{\cdot}10^{-6}$ | ... | $16.1{\cdot}10^{-6}$ | $16.1{\cdot}10^{-6}$ |
| $\alpha_{CA}$ | (13) | $22.0{\cdot}10^{-6}$ | $23.2{\cdot}10^{-6}$ | ... | $22.8{\cdot}10^{-6}$ | $22.8{\cdot}10^{-6}$ |
| $Ra_{CA}$ | (10) | $0.8{\cdot}10^{7}$ | $3.1{\cdot}10^{7}$ | ... | $2.4{\cdot}10^{7}$ | $2.4{\cdot}10^{7}$ |
| $Nu_{CA}$ | (19) | 28.6 | 40.5 | ... | 37.9 | 37.9 |
| $h_{conv-CA}$ | (7) | 2.9391 | 4.2694 | ... | 3.9655 | 3.9655 |
| $R_{conv-CA}$ | (8) | 0.1831 | 0.1261 | ... | 0.1357 | 0.1357 |
| $h_{rad-CA}$ | (24) | 1.2083 | 1.3228 | ... | 1.2832 | 1.2832 |
| $R_{rad-CA}$ | (25) | 0.4454 | 0.4069 | ... | 0.4194 | 0.4194 |
| $R_3$ | (8)‖(25) | 0.1298 | 0.0962 | ... | 0.1025 | 0.1025 |
| $Q_t$ | (28) | 38.5 | 239.2 | ... | 165.2 | 165.2 |
| $T_{f-BA}$ | (12) | 25.5 | 36.4 | ... | 32.5 | 32.8 |
| $\beta_{BA}$ | (11) | 0.0033 | 0.0032 | ... | 0.0033 | 0.0033 |
| $\rho_{BA}$ | (15) | 1.1819 | 1.1403 | ... | 1.1550 | 1.1539 |
| $k_{BA}$ | (14) | 0.0261 | 0.0269 | ... | 0.0266 | 0.0266 |
| $\mu_{BA}$ | (17) | $18.4{\cdot}10^{-6}$ | $18.9{\cdot}10^{-6}$ | ... | $18.7{\cdot}10^{-6}$ | $18.7{\cdot}10^{-6}$ |
| $\nu_{BA}$ | (16) | $15.7{\cdot}10^{-6}$ | $16.6{\cdot}10^{-6}$ | ... | $16.2{\cdot}10^{-6}$ | $16.2{\cdot}10^{-6}$ |
| $\alpha_{BA}$ | (13) | $22.0{\cdot}10^{-6}$ | $23.5{\cdot}10^{-6}$ | ... | $22.9{\cdot}10^{-6}$ | $23.0{\cdot}10^{-6}$ |
| $Ra_{BA}$ | (10) | $0.8{\cdot}10^{7}$ | $3.6{\cdot}10^{7}$ | ... | $2.7{\cdot}10^{7}$ | $2.8{\cdot}10^{7}$ |
| $Nu_{BA}$ | (19) | 14.3 | 20.9 | ... | 19.4 | 19.6 |
| $h_{conv-BA}$ | (7) | 1.4696 | 2.2139 | ... | 2.0361 | 2.0515 |
| $R_{conv-BA}$ | (8) | 0.3662 | 0.2431 | ... | 0.2643 | 0.2623 |
| $h_{rad-BA}$ | (24) | 1.2083 | 1.3481 | ... | 1.2959 | 1.2998 |
| $R_{rad-BA}$ | (25) | 0.4454 | 0.3992 | ... | 0.4153 | 0.4141 |
| $R_4$ | (8)‖(25) | 0.2010 | 0.1511 | ... | 0.1615 | 0.1606 |
| $Q_b$ | (30) | 24.9 | 177.5 | ... | 117.1 | 121.5 |
| $T_{f-SA}$ | (12) | 25.5 | 36.4 | ... | 32.5 | 32.8 |
| $\beta_{SA}$. | (11) | 0.0033 | 0.0032 | ... | 0.0033 | 0.0033 |
| $\rho_{SA}$ | (15) | 1819 | 1.1403 | ... | 1.1550 | 1.1539 |
| $k_{SA}$ | (14) | 0.0261 | 0.0269 | ... | 0.0266 | 0.0266 |
| $\mu_{SA}$ | (17) | $18.4{\cdot}10^{-6}$ | $18.9{\cdot}10^{-6}$ | ... | $18.7{\cdot}10^{-6}$ | $18.7{\cdot}10^{-6}$ |
| $\nu_{SA}$ | (16) | $15.7{\cdot}10^{-6}$ | $16.6{\cdot}10^{-6}$ | ... | $16.2{\cdot}10^{-6}$ | $16.2{\cdot}10^{-6}$ |
| $\alpha_{SA}$ | (13) | $22.0{\cdot}10^{-6}$ | $23.5{\cdot}10^{-6}$ | ... | $22.9{\cdot}10^{-6}$ | $23.0{\cdot}10^{-6}$ |
| $Ra_{SA}$ | (10) | $0.5{\cdot}10^{6}$ | $2.3{\cdot}10^{7}$ | ... | $1.7{\cdot}10^{7}$ | $1.8{\cdot}10^{7}$ |
| $Pr_{SA}$ | (18) | 0.7092 | 0.7064 | ... | 0.7074 | 0.7073 |
| $Nu_{SA}$ | (20) | 14.4 | 20.7 | ... | 19.3 | 19.4 |
| $h_{conv-SA}$ | (7) | 3.6937 | 5.4793 | ... | 5.0525 | 5.0895 |
| $R_{conv-SA}$ | (8) | 0.8742 | 0.5893 | ... | 0.6391 | 0.6345 |
| $h_{rad-SA}$ | (24) | 1.2083 | 1.3481 | ... | 1.2959 | 1.2998 |
| $R_{rad-SA}$ | (25) | 2.6724 | 2.3953 | ... | 2.4918 | 2.4844 |
| $R_6$ | ((8)‖(25))/2 | 0.3294 | 0.2365 | ... | 0.2543 | 0.2527 |
| $Q_s$ | (31) | 15.2 | 113.4 | ... | 74.4 | 77.2 |
| | | Step 2 | | | | |
| $S$ | (5) | 82.5271 | 82.5271 | ... | 82.5271 | 82.5271 |
| $R_1$ | (2) | 0.0606 | 0.0606 | ... | 0.0606 | 0.0606 |
| $T_{surf}$ | (26) | 76.7 | 64.5 | ... | 69.0 | 69.0 |
| | | Step 3 | | | | |
| $T_f$ | (12) | 52.3 | 55.3 | ... | 54.5 | 54.5 |
| $\beta$ | (11) | 0.0031 | 0.0030 | ... | 0.0031 | 0.0031 |
| $\rho$ | (15) | 1.0845 | 1.0748 | ... | 1.0774 | 1.0774 |
| $k$ | (14) | 0.0281 | 0.0284 | ... | 0.0283 | 0.0283 |
| $\mu$ | (17) | $19.6{\cdot}10^{-6}$ | $19.8{\cdot}10^{-6}$ | ... | $19.7{\cdot}10^{-6}$ | $19.7{\cdot}10^{-6}$ |
| $\nu$ | (16) | $18.1{\cdot}10^{-6}$ | $18.4{\cdot}10^{-6}$ | ... | $18.3{\cdot}10^{-6}$ | $18.3{\cdot}10^{-6}$ |
| $\alpha$ | (13) | $25.8{\cdot}10^{-6}$ | $26.2{\cdot}10^{-6}$ | ... | $26.1{\cdot}10^{-6}$ | $26.1{\cdot}10^{-6}$ |
| $Ra$ | (10) | $3.9{\cdot}10^{5}$ | $1.4{\cdot}10^{5}$ | ... | $2.3{\cdot}10^{5}$ | $2.3{\cdot}10^{5}$ |
| $Pr$ | (18) | 0.7024 | 0.7017 | ... | 0.7019 | 0.7019 |
| $Nu$ | (9) | 4.9241 | 3.5168 | ... | 4.1041 | 4.1041 |
| $h_{conv}$ | (7) | 2.7693 | 1.9933 | ... | 2.3213 | 2.3213 |

TABLE XIV: (CONTINUED)

| | | | | | | |
|---|---|---|---|---|---|---|
| $R_{conv}$ | (8) | 0.1943 | 0.2700 | ... | 0.2319 | 0.2319 |
| $h_{rad}$ | (22) | 0.7289 | 0.7452 | ... | 0.7406 | 0.7406 |
| $R_{rad}$ | (23) | 0.7384 | 0.7222 | ... | 0.7267 | 0.7267 |
| $R_2$ | (8)‖(23) | 0.1539 | 0.1965 | ... | 0.1758 | 0.1758 |
| $Q_t$ | (27) | 239.2 | 154.7 | ... | 165.2 | 165.2 |
| | | Step 4 | | | | |
| $S$ | (5) | 2.8740 | 2.8740 | ... | 2.8740 | 2.8740 |
| $R_5$ | (2)/2 | 0.8699 | 0.8699 | ... | 0.8699 | 0.8699 |
| $T_{cover}$ | (32) | 46.0 | 39.0 | ... | 39.4 | 39.4 |
| $T_{b\&s}$ | (33) | 49.8 | 37.1 | ... | 42.5 | 42.1 |
| | | Step 5 | | | | |
| $\lvert E_{cover}\rvert$ | (34) | 100 | 18.0 | ... | 0.0 | 0.0 |
| $\lvert E_{b\&s}\rvert$ | (35) | 100 | 21.8 | ... | 0.6 | 0.4 |
| | | Total generated heat & current | | | | |
| $Q$ | (36) | 279.3 | 445.6 | ... | 356.7 | 364.0 |
| $I$ | (37) | 136 | 172 | ... | 154 | 155 |

## REFERENCES


[1] Mono-Systems. 2016. Solid bottom cable tray system. [Online]. Available: http://www.monosystems.com/products/item/trough-tray/129/10017

[2] SpecMate Wireway Systems. SPM series—solid bottom cable tray system, Feb. 2005. [Online]. Available: http://www.cs.unc.edu/sittsouth/network/product_cut_sheets/ed579

[3] R. V. Rebbapragada, D. O'Neill, M. Zuzovsky, and R. Weronick, "Ampacity of cables in solid bottom trays with and without covers," in *Proc. Conf. Rec. IEEE Nuclear Sci. Symp.*, 1999, vol. 3, pp. 1704–1707.

[4] Cable Tray Institute. 2016. Cable tray type selection. [Online]. Available: http://www.cabletrays.org/pdfs/Cabletrays-Institute-Technical-Bulletin4.pdf

[5] J. Stolpe, "Ampacities for cables in randomly filled cable trays," *IEEE Trans. Power App. Syst.*, vol. PAS-90, no. 3, pp. 962–974, May 1972.

[6] G. Engmann, "Ampacity of cable in covered tray," *IEEE Trans. Power App. Syst.*, vol. PAS-103, no. 2, pp. 962–974, Feb. 1984.

[7] B. L. Harshe and W. Z. Black, "Ampacity of cables in single open-top cable trays," *IEEE Trans. Power Del.*, vol. 9, no. 4, pp. 1733–1740, Oct. 1994.

[8] B. L. Harshe and W. Z. Black, "Ampacity of cables in single covered trays," *IEEE Trans. Power Del.*, vol. 12, no. 1, pp. 3–14, Jan. 1997.

[9] W. Z. Black and B. L. Harshe, "Ampacity of diversely loaded cables in covered and uncovered trays," *IEEE Trans. Power Del.*, vol. 15, no. 1, pp. 3–7, Jan. 2000.

[10] ICEA/NEMA ampacities of cables installed in cable trays, ICEA Publ. No. P-54-440; NEMA publ. no. WC51, NEMA, Washington, DC, USA, 1986.

[11] S.-B. Liu and X. Han, "Analytical method of calculating the transient and steady-state temperature rises for cable-bundle in tray and ladder," *IEEE Trans. Power Del.*, vol. 13, no. 3, pp. 691–698, Jul. 1998.

[12] NFPA-70, National Electric Code, 2014.

[13] F. P. Incropera and D. P. DeWitt, *Introduction to Heat Transfer*, 3rd ed. Hoboken, NJ, USA: Wiley, 1996, p. 698.

[14] M. M. Yovanovich, "A general expression for predicting conduction shape factors," in *Proc. AIAA 11th Aerosp. Sci. Meeting*, Jan. 1973, pp. 266–291.

[15] S. S. Kutateladze and V. M. Borishanskii, *A Concise Encyclopedia of Heat Transfer*. Cambridge, MA, USA: Pergamon Press, 1966.

[16] W. M. Rohsenow, J. P. Harnett, and Y. I. Cho, *Handbook of Heat Transfer*, 3rd ed. New York, NY, USA: McGraw-Hill, 1998.

[17] J. H. Lienhard IV and J. H. Lienhard V, *A Heat Transfer Textbook*, 3rd ed. Cambridge, MA, USA: Phlogiston Press, 2008.

[18] M. Terracciano, S. Purushotaman, F. de León, and A. R. Farahani, "Thermal analysis of cables in unfilled troughs: Investigation of the IEC standard and a methodological approach for cable thermal rating," *IEEE Trans. Power Del.*, vol. 27, no. 3, pp. 1423–1431, Jul. 2012.

[19] General Cable. Apr. 2015. Spec. [Online]. Available: http://www.generalcable.com/na/us-can/products-solutions/industrial/medium-voltage-cable/copper-tape-shielded-type-mv-cable

[20] The Engineering ToolBox. 2016. Emissivity coefficients of some common materials. [Online]. Available: http://www.engineeringtoolbox.com/emissivi ty-coefficients-d_447.html


Authors,' photographs and biographies not available at the time of publication.